

A CRYOCOOLED NORMAL-CONDUCTING AND SUPERCONDUCTING HYBRID CW PHOTOINJECTOR

H. Qian[#], M. Krasilnikov, F. Stephan, DESY, Zeuthen, Germany

Abstract

Continuous wave (CW) photoinjectors have seen great progress in the last decades, such as DC gun, superconducting RF (SRF) gun and normal conducting (NC) VHF-band gun. New developments of CW guns are aiming higher acceleration gradient and beam energy for higher beam brightness. While a SRF gun being the natural CW gun technology for better performance, it has been technically limited by the compatibility between normal conducting high QE cathodes and superconducting (SC) cavity. In this paper, a high gradient and low voltage cryocooled CW NC gun is proposed to house the high QE cathode, and a half cell SRF cavity immediately nearby gives further energy acceleration. Preliminary RF design of the NC gun and ASTRA simulations of such a hybrid photoinjector are presented.

INTRODUCTION

Electron sources of both high peak brightness and high average brightness are wished for a lot of advanced applications [1]. Pulsed electron guns enjoy a high cathode gradient (60-200 MV/m), enabling electron beams with high 6D-brightness possible right at the cathode. Such high gradients are difficult to extend to a CW gun, due to cooling concerns, dark current, and other concerns. Current CW RF guns operate at cathode gradient around 20 MV/m [2,3], and beam transverse brightness are optimized by relaxing peak current at photoemission, which is recovered by velocity bunching or magnetic bunch compression [4,5]. To achieve higher beam brightness, higher cathode gradient and beam energy is wished [1]. The next generation of normal conducting VHF-band gun with over 30-MV/m cathode gradient is under study, and a major challenge is thermal loading (over 100 kW)[6].

Based on such a gun design, ASTRA simulations have shown that the emittance of a 100-pC beam can be improved towards $\sim 0.1 \mu\text{m}\cdot\text{rad}$ [6,7]. Besides, SRF guns have made great progress in the past decade, showing the possibility of high cathode gradient up to 60 MV/m [8]. The compatibility of a high-QE cathode and a high gradient SRF cavity is still a technical challenge. In most of cases, the SRF gun gradient is greatly reduced once a high QE photocathode is present inside the cavity. Besides, multipacting inside the gun can also kill the high QE cathode [9]. While engineering improvements have been implemented in the design of cathode insertion channels of SRF guns to mitigate multipacting and to avoid cathode contamination to SRF cavity surface, risks still exist due to the high sensitivity of SRF cavity surface.

Other special SRF gun designs are also under development. The DESY 1.5-cell L-band SRF gun uses superconducting metal cathodes, eliminating the gap between SRF cavity and NC high QE cathodes for potentially high-gradient performance [8]. The DC-SRF gun developed at Peking University puts the high-QE cathode inside the DC gun just before the SRF cavity, preventing the complex cathode channel design and cathode contamination to SRF cavity. The DC-SRF gun has demonstrated an average current of $\sim \text{mA}$ for CW operation [10].

Inspired by the DC-SRF gun, the DC acceleration of the hybrid gun is proposed to be replaced by a high-gradient NC-CW RF gun, forming a NC-SRF gun, so that beam brightness is not limited by the low cathode gradient. In this paper, the preliminary concept and RF design of such a gun is described, and the engineering considerations are not discussed. Based on the proposed NC-SRF gun concept, a CW photoinjector is optimized by ASTRA simulations.

NC-SRF GUN CONCEPT

The high gradient NC RF cavity is proposed to house the high QE cathode and support high brightness photoemission with high cathode gradient, and the main acceleration is still in the SRF cavity. The compatibility between high gradient NC RF cavity and high QE cathode has been well demonstrated in both pulsed and CW NC guns [11,12]. Since the NC cavity voltage is supposed to be low, to maintain the beam brightness from the NC cavity, the SRF cavity should be as close to the NC cavity as possible, same as in the DC-SRF gun. Since the NC cavity and SRF cavity will stay in the same cryomodule, the NC cavity should be cryocooled, and then the NC cavity RF heating should be minimized. The NC cavity should be high gradient with low cavity voltage, i.e. a thin gap cavity. A re-entrant cavity shape is considered for such a thin gap cavity. Scaling from the existing LBL VHF gun parameters [3], i.e. $\sim 100 \text{ kW}$ for 800 kV, the gun is assumed to be $\sim 1 \text{ kW}$ for 80 kV. Since the NC cavity will be cryocooled, the cavity quality factor will increase, and the RF heating will be even lower. Several cryocooled NC guns have been proposed for the purpose of ultrahigh gradient operation [13,14]. Microwave measurements at cryogenic temperature (20 K) has shown RF surface-resistance reduction of a factor of ~ 5 compared to room temperature at both S-band and C-band frequencies [15,16]. Applying the same reduction ratio to the assumed 80 kV NC cavity, the RF heating, i.e. cryogenic load at 20 K will be reduced from $\sim 1 \text{ kW}$ to $\sim 200 \text{ W}$.

[#]houjun.qian@desy.de

To keep the NC cavity RF heating low and RF energy curvature small for a sub-100 ps beam, a low frequency cavity, i.e. sub-harmonic of 1.3 GHz, is designed. To have a thin gap low frequency cavity with compact cavity size, the re-entrant cavity shape is used. The SRF cavity for main acceleration has many options, such as single cell or multi cell, 1.3 GHz or its sub harmonic. For the first design, a half-cell 1.3-GHz SRF cavity is used. Both the low frequency NC cavity and the half-cell SRF cavity are designed using the SUPERFISH code.

Figure 1 shows a preliminary physics design without engineering realizations, and both cavity designs are not fully optimized yet from RF and beam dynamics perspectives. The separation between the two cavities is chosen arbitrarily without consulting engineers, and the half-cell SRF cavity front wall is 37.3 mm from cathode.

The NC cavity frequency is 325 MHz, and shunt impedance is 4.27 M Ω at room temperature. With a 30 MV/m gradient on the cathode, the cavity voltage is \sim 80 kV, and the cavity RF heating at room temperature is \sim 1.5 kW, which is a bit worse than the scaling from the LBL VHF cavity (185.7 MHz) [3]. With further cavity optimizations, the cavity shunt impedance is expected to increase. The on-axis electric field maps of both cavities are shown in Fig. 2. If both the NC and SC cavity peak gradients are assumed to be 30 MV/m, the total beam energy acceleration is \sim 1.4 MeV.

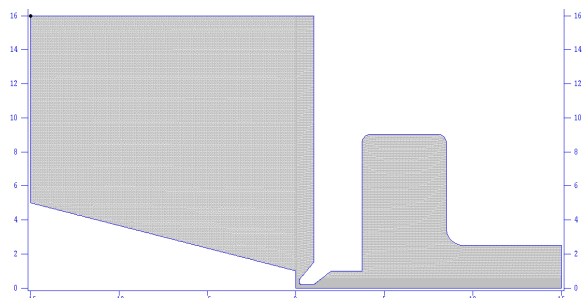


Figure 1: Preliminary SUPERFISH model of a NC-SRF gun, consisting of a re-entrant NC cavity (325 MHz) and a half-cell SRF cavity (1.3 GHz).

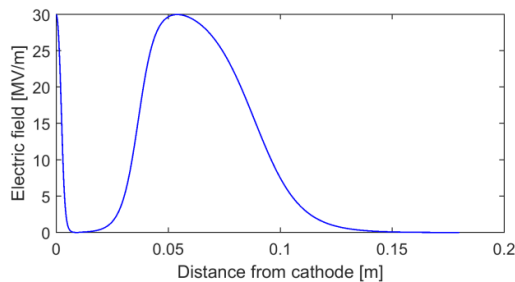


Figure 2: On-axis electric field of the NC-SRF gun in Fig. 1. The two cavities are de-coupled, and the field amplitudes in the plot are preliminary assumptions.

Further RF optimizations have to be done, and beam dynamics verifications of such a gun concept are shown in the next section.

BEAM DYNAMICS OPTIMIZATION

A classical photoinjector layout based on the NC-SRF gun is shown in Fig. 3, consisting of the gun, a SC solenoid, and an 8-cavity cryomodule (CM). Other photoinjector layouts, including a dedicated buncher cavity and two solenoids, are not yet tested in this paper.



Figure 3: Preliminary photoinjector layout.

The photoinjector is optimized using a multi-objective genetic algorithm (MOGA). A code developed at LBL can be used to drive ASTRA simulations for searching optimal solutions of both good emittance and short bunch length [17]. In this paper, only emittance is optimized, no constraint on bunch length is done in the optimizations for simplicity. Two cases are simulated with a 100 pC bunch charge. In the first case, phase of cavity #1 in the 8-cavity CM is allowed to vary for velocity bunching. In the 2nd case, phase of cavity #1 is set to on-crest.

The peak gradients of the NC and SC cavity are fixed at 30 MV/m, which are a bit higher than current operating cavities (\sim 20 MV/m). The 2nd and 3rd cavities in the 8-cavity CM are OFF, following the LCLS-II injector experience [18]. The 4th cavity amplitude is variable, and all the other cavities in the module are set to fixed amplitudes of 32 MV/m with on-crest phases. The laser is a quasi-flat-top distribution. The transverse distribution is a Gaussian distribution with 1-sigma cut, and the longitudinal distribution is a flat-top with 2-ps rising and falling edges. The cathode thermal emittance is assumed to be 0.5 μ m.rad/mm.

There are 9 variable parameters during the optimization for the case with velocity bunching by cavity #1 in CM, which are listed in Table 1. For the 2nd case without velocity bunching, there are 8 variables, excluding the cavity #1 phase.

Content from this work may be used under the terms of the CC BY 3.0 licence (© 2018). Any distribution of this work must maintain attribution to the author(s), title of the work, publisher, and DOI.

Table 1: Nine Variable Parameters During Photoinjector Optimizations (for the case including velocity bunching)

Parameter	Range	Unit
SC cavity phase	[-10, 10]	degree
Solenoid peak field	[0, 0.1]	T
Solenoid position	[0.55, 1.5]	m
1 st cavity position in CM	[2, 5]	m
1 st cavity amplitude	[0, 32]	MV/m
1 st cavity phase	[-90, 0]	degree
4 th cavity amplitude	[0, 32]	MV/m
Laser radius	[0.1, 1.5]	mm
Laser pulse duration	[10, 70]	ps

Two solutions with best emittance results at the end of photoinjector are found, without touching the hard limits in Table 1. The emittance results are listed in Table 2. The current profiles and slice emittances are shown in Fig. 4 and Fig. 5. The longitudinal phase spaces after removing linear and quadratic energy chirps are plotted in Fig. 6.

Although the emittance values from the two optimal solutions are low, many other aspects of the beam indicate the injector is still not optimum. Emittance decompositions [19], in Table 2, show both beams are not thermal emittance dominated, which should be a feature of state of the art photoinjector optimizations [20]. Emittance growth from slice mismatch and slice emittance growth are large compared to thermal emittance. In the longitudinal phase space, both beam current profiles are highly distorted, and the higher order energy spread of the beam with velocity bunching is high. Both transverse and longitudinal phase space analysis show the injector is still not optimum. Both the NC-SRF gun and the injector layout need further optimizations.

Table 2: Emittance decomposition for solutions shown in Figs. 4 and 5. $\epsilon_{100\%}$ is 100% projected emittance, $\epsilon_{95\%}$ is 95% projected emittance, $\langle \epsilon_{\text{slice}} \rangle$ is average slice emittance, ϵ_{th} is thermal emittance, $\Delta \epsilon_{\text{mis}}$ is projected emittance growth from longitudinal-slice mismatch, and $\Delta \epsilon_{\text{slice}}$ is slice emittance growth w.r.t. thermal emittance.

	No chirp in Cav 1	Chirp in Cav 1	Unit
$\epsilon_{100\%}$	0.31	0.20	μm
$\epsilon_{95\%}$	0.24	0.13	μm
$\langle \epsilon_{\text{slice}} \rangle$	0.23	0.13	μm
ϵ_{th}	0.08	0.06	μm
$\Delta \epsilon_{\text{slice}}$	0.22	0.12	μm
$\Delta \epsilon_{\text{mis}}$	0.20	0.15	μm

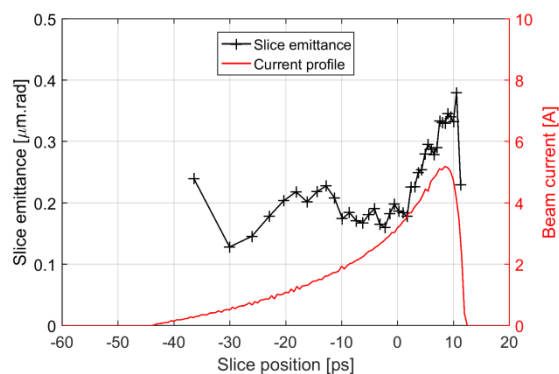


Figure 4: Slice emittance and current profile for 100 pC beam based on the injector in Fig. 3, no velocity bunching by cavity #1 of 8-cavity CM.

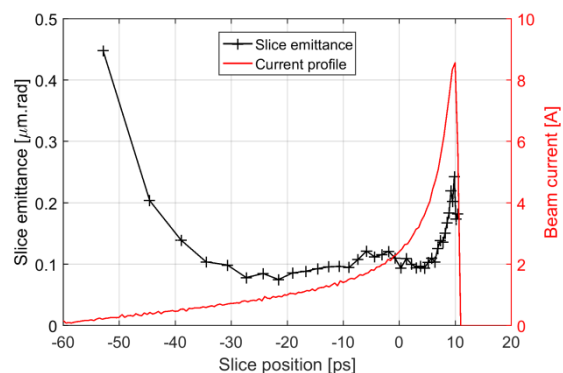


Figure 5: Slice emittance and current profile for 100 pC beam based on the injector in Fig. 3, with velocity bunching by cavity #1 of 8-cavity CM.

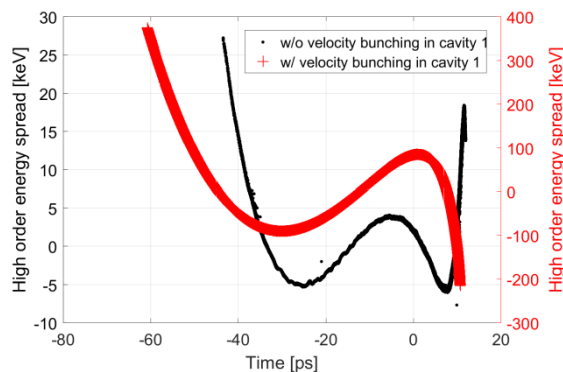


Figure 6: Longitudinal phase space of the two solutions in Figs. 4 and 5 after removing the linear and quadratic energy chirps, showing a 4.4-keV (rms) higher-order energy spread for the case w/o velocity bunching (left axis), and a 76-keV (rms) higher-order energy spread for the case w/ velocity bunching (right axis).

Although the injector is still not optimized, the low thermal emittances in both solutions indicate high transverse beam brightness from photoemission, which supports the considerations of a high gradient but low voltage cathode cell design.

CONCLUSION

In this paper, a cryocooled NC-SRF gun concept is proposed. A high gradient and low voltage NC cathode cell not only simplifies the normal conducting high QE cathode compatibility issues in SC gun, but also supports the high transverse brightness photoemission. A SC cavity immediately nearby will do the main acceleration to damp the space charge effect and conserve the beam brightness from the cathode cell. The two cavities are decoupled.

A preliminary gun concept is designed by SUPERFISH code. Preliminary beam dynamics optimizations based on such a gun with 30 MV/m in both the NC cathode cell and SC cell are presented for a bunch charge of 100 pC. Although low emittance values are found, analysis of both transverse and longitudinal phase spaces show the injector is still not optimum. Both the gun concept and the injector layout need further developments.

REFERENCES

- [1] *Report of the Basic Energy Sciences Workshop on the Future of Electron Sources*: https://science.energy.gov/~media/bes/pdf/reports/2017/Future_Electron_Source_Worskhop_Report.pdf
- [2] R. Xiang, in *Proc. IPAC'17*, p. 500.
- [3] F. Sannibale *et al.*, *PRST-AB* 15, 103501 (2012).
- [4] I. Bazarov *et al.*, *PRST-AB* 8, 034802 (2005).
- [5] D. Filippetto *et al.*, *PRST-AB* 17, 024201 (2014).
- [6] F. Sannibale *et al.*, in *Proc. IPAC'17*, p. 542.
- [7] H. Qian *et al.*, presented at FEL'17, this conference.
- [8] J. Sekutowicz, in *Proc. SRF'15*, p. 994.
- [9] I. Petrushina *et al.*, in *Proc. IPAC'17*, p. 1180.
- [10] K. Liu *et al.*, presented at FEL'17, this conference.
- [11] D. Filippetto *et al.*, *Appl. Phys. Lett.* 107 042104 (2015).
- [12] M. Krasilnikov *et al.*, *PRST-AB* 15, 100701 (2012).
- [13] V. Vogel *et al.*, in *Proc. IPAC'11*, p. 77.
- [14] J. Rosenzweig *et al.*, arXiv:1603.01657.
- [15] A. Cahill *et al.*, in *Proc. IPAC'16*, p. 487.
- [16] T. Tanaka *et al.*, in *Proc. IPAC'17*, p. 518.
- [17] C. F. Papadopoulos *et al.*, in *Proc. FEL'14*, p. 864.
- [18] C. Mitchell *et al.*, in *Proc. IPAC'16*, p. 1699.
- [19] C. Mitchell, arXiv:1509.04765.
- [20] C. Gulliford *et al.*, *Appl. Phys. Lett.* 106, 094101 (2015).